

<https://doi.org/10.48047/AFJBS.4.4.2022.327-354>



African Journal of Biological Sciences

Journal homepage: <http://www.afjbs.com>



Research Paper

Open Access

“Identification of potential pyridyltriazole derivatives for Mtb enoyl-reductase InhA inhibition through *in silico* molecular docking and ADMET study.”

Ashish K. Mullani^{1*}, Manoj S. Charde²

1 Department of Pharmaceutical Chemistry, Annasaheb Dange College of B. Pharmacy, Ashta, 4166301, Maharashtra, India

2. Department of Pharmaceutical Chemistry, Government College of Pharmacy, Karad, 415124, Maharashtra, India

E-mail: mullani.ashishadcbp@gmail.com

Mobile No- 8600732013

ORCID iD: 0009-0004-5906-7426

Department of Pharmaceutical Chemistry, Government College of Pharmacy, Karad, Maharashtra

E-mail: manojjudps@rediffmail.com

Mobile No- 7350555124

ORCID iD: 0009-0004-5906-7426

Correspondence to Author: Prof. Ashish K. Mullani

Department of Pharmaceutical Chemistry, Annasaheb Dange College of Pharmacy, Ashta, Tal- walwa, DistSangli – 416301, Maharashtra, India. E-mail: mullani.ashishadcbp@gmail.com

Mobile No- 800732013

ORCID iD: 0009-0004-5906-7426

Volume 4, Issue 4, April 2022

Received: 15 Mar 2022

Accepted: 05 April 2022

Published: 25 April 2022

[doi: 10.48047/AFJBS.4.4.2022.327-354](https://doi.org/10.48047/AFJBS.4.4.2022.327-354)

Abstract-

In the current investigation, Tuberculosis remains a formidable global health challenge, necessitating innovative approaches for effective treatment. Current study attempted to identify potential pyridyltriazole derivatives for Mtb enoyl-reductase InhA inhibition from virtually designed ligand library. Molecular docking study was utilized for identification of hits against selected molecular target. This *in silico* study delved into the molecular interactions between potential compounds and the Mtb enoyl-reductase InhA (PDB 5JFO). Furthermore, research utilising molecular docking have been conducted to get mechanistic understanding and molecular interactions in opposition to the mycobacterial InhA enzyme. Utilising a molecular docking analysis, hits against specific molecular targets were found. Compound 21 emerged with the highest negative binding affinity (-10.2kcal/mol) further followed closely by compound 5 (-10.1 kcal/mol) and found exhibiting promising interactions within the active site of enoyl-reductase InhA. According to the In-silico ADME prediction, every designed molecule has drug-like qualities and is appropriate for oral bioavailability. These findings emphasize the potential of these compounds as inhibitors and place the footing for further optimization to develop more potent anti-TB therapeutics.

Keywords: *In silico*, Molecular docking, *Mycobacterium tuberculosis*, Tuberculosis, Mtb enoyl-reductase InhA

1. OVERVIEW-

One of the deadliest and oldest infectious diseases is tuberculosis (TB), which is brought on by the *Mycobacterium tuberculosis* (Mtb)¹. Tuberculosis caused by Mtb remains a persistent global human health threat and continues to pose threat with a significant impact on morbidity and mortality worldwide². According to the World Health Organization's 2022 global tuberculosis report, 10.6 million new cases of tuberculosis were expected to have caused almost 1.6 million deaths globally in 2013.³ The burden of TB in India persists as a significant public health challenge highlighting its global prevalence and the alarming incidence of drug-resistant cases within the country⁴. India is one of the top eight countries responsible for more than two-thirds of the world's TB cases as of 2020⁵. The majority of drug-resistant tuberculosis cases worldwide are also found in India. In addition, statistics indicate that India accounts for one in four global cases of multidrug-resistant tuberculosis (MDR-TB). An estimated 119,000 MDR-TB infections were recorded in India in 2021^{6, 7}. However, these numbers may be greatly underestimated due to testing constraints and the fact that only 76% of newly diagnosed TB cases and 73% of patients who previously underwent treatment have been evaluated for rifampicin resistance⁶. In India, the number of patients who were further started on treatment for MDR-TB and extensively drug-resistant (XDR)-TB was remarkably low, at 4 per 100,000 and 1 per 100,000 in 2021, respectively.⁸⁻¹⁰. Alarming, the overall success rates of TB treatment in India were suboptimal and stood at 57 percent in 2019. These concerning statistics from India underscore the urgent need for improved testing, appropriate treatment, and enhanced strategies to combat drug-resistant TB¹¹.

Enoyl-reductase InhA is one of the key enzymes essential for the survival of Mtb¹². Mycolic acid production, an essential part of the mycobacterial cell wall, depends on InhA¹³. For the production of mycolic acid and the integrity of the bacterial cell wall, InhA catalyzes the last step of fatty acid elongation and reduces double bonds in fatty acids^{6, 14}.

Isoniazid, a first-line anti-TB medication, targets it to decrease its function and interfere with the formation of mycolic acid¹⁵. The necessity of comprehending the complex mechanisms controlling InhA and its involvement in drug resistance, however, has been emphasized by the rise of drug-resistant strains¹⁶. The current work used docking study to in silico identify possible hits against Mtb enoyl-reductase InhA¹⁷. One can determine the medications' binding orientation and affinity towards their specific targets by utilizing the results of a molecular docking investigation¹⁸.

2. Material and Methods

***insilico* docking study -**

2.1 Ligand preparation

Using ACD/Chemdraw software, the chemical structures and SMILES of the designed compounds were created [19]. In order to rectify the tautomeric and ionization states, produced structures were protonated using BIOVIA Discovery Studio [20]. The Avogadro program was utilized to minimize energy in the created chemical structures [21]. The force field MMFF94 with the steepest descent algorithm was applied to the developed compounds in order to minimize their energy [22]. The structure of the newly designed ligands was drawn (Table 1).

2.2 Protein preparation

The RCSB Protein Data Bank²³ provided the previously published crystal form structure of Mtb enoyl-reductase InhA (PDB 5JFO), which has a resolution of 2.91 Å [26]. All of the het atoms and water molecules were eliminated from the downloaded protein crystal structure in order to improve it for docking study [27]. To protonate the residues of amino acids in a pristine protein crystal structure, polar hydrogen atoms were added²⁶. The protein structure enhancement protocol was performed using BIOVIA Discovery Studio [20].

2.3 Molecular docking-

Virtually designed compounds were subjected to docking study against (PDB 5JFO). Docking protocol was executed using the PyRx 0.8 program²⁶. The AutoDockVina wizard unit of PyRx 0.8 was used to import and choose prepared protein and ligand structures²⁷. The blind docking protocol was used to explore the binding ability of docked compounds on entire protein surface^{28, 29}. Grid box was focused at center coordinates as X: -38.776, Y: -29.025, Z: 25.0202 and the dimension of grid was selected as X: 93.7654, Y: 92.0372, Z: 73.3332 coordinates. By default, the exhaustiveness was set to 8^{30, 31}. Each compound's docked pose with the highest negative binding affinity was stored in pdb format, and BIOVIA Discovery Studio was used to examine other binding interactions [32-35].

2.4 Drug likeness properties

The physicochemical properties of designed pyridyltriazole derivatives (1–24) were evaluated in accordance with established rules to determine their drug-likeness. Veber's rule and Lipinski's rule of five were used in this investigation to assess the drug-likeness features. To determine the drug-likeness and ADMET profile of designed compounds, several critical factors were examined, including molecular weight, lipophilicity, hydrogen bond donors and acceptors, molecular refractivity, topological polar surface area, and number of rotatable bonds in the drug-likeness. **SwissADME** was used for the to determine their drug-likeness [11-15].

2.5 Predicted ADME Study-

The Pharmacokinetics properties are determined by using the ADMETSar and & pkCSM server. The pharmacokinetics properties include adsorption, distribution, metabolism and excretion.

ADMET parameters were predicted using admetSAR 3.0 & pkCSM web server [23]. ADME parameters such as water solubility, CaCo2 permeability, intestinal absorption, P-glycoprotein, volume of distribution, blood brain barrier (BBB) and CNS permeability along with Toxicity parameters such as AMES toxicity (mutagenicity) and Hepatotoxicity [27] were predicted [11-15].

3. Results & Discussion-

3.1 Molecular docking-

The molecular docking of the designed molecules i.e. pyridyltriazole derivatives are docked with the 5JFO protein of the InHA enzyme (2-trans-enoyl-acyl carrier protein reductase). The binding affinity of the compounds is observed between the ranges of -10.2 to -7.1. Amongst all the twenty four molecules 1,3,5,11,16,21& 22 was observed to be the most potent molecule with the docking score of -9.7, -9.4, -10.1, -8.0, -8.2,-10.2 7 -9.3 respectively.

The negative binding affinities reflected the thermodynamic favorability of binding interactions indicating a potentially stable complex formation between Compound 21 and the targeted enzyme. Compound 21 demonstrated the highest negative binding affinity with value of -10.2 kcal/mol. Compound 21 formed a Conventional Hydrogen Bond with ILE21, SER 20, SER 94 AND VAL 65 at a bond distance of 3.33, 2.91, 3.24, 3.30, 3.46Å (Table-2) respectively. Compound 21 established a π -Sigma bond with ILE 95 while this residue was also involved in forming diverse interactions including π - π Stacked, π -Donor Hydrogen Bond with Compound 21. Amino acid residues such as PHE 41 AND PHE 97 participated in the formation of π - π Stacked and π -Donor Hydrogen Bond interactions with Compound 21. The 3D binding orientation of Compound 21 with Mtb enoyl-reductase InhA (PDB 5JFO) was depicted in (Figure-1). The diverse interactions described between Compound 21 and the amino acid residues of InhA highlighted its possible potential as a strong inhibitor.

Additionally, compound 5 exhibited the second-highest negative binding affinity of -10.1 kcal/mol against Mtb enoyl-reductase InhA (PDB 5JFO). Binding profile compound 5 showed formation of a carbon-hydrogen interaction with ILE 21, SER 20, along with a π -Stacked bond with the PHE 41, PHE 97 residue. Furthermore, a π -Donor Hydrogen Bond binding interaction was observed between compound 5 and THR 197. Compound 5 engaged in π -Alkyl interactions with multiple amino acid residues, namely ILE 95, ILE 122 and ALA 198. Formation of diverse range of interactions demonstrated by compound 5 with specific amino acid residues within the active site of InhA underscores its possibility of potential as a potent inhibitor. The formation of specific interactions like Conventional Hydrogen Bond, π -Sigma, π - π Stacked and π -Donor Hydrogen Bond interactions may play a significant role in the molecular recognition and binding of small molecules with their respective TB targets (Figure-2).

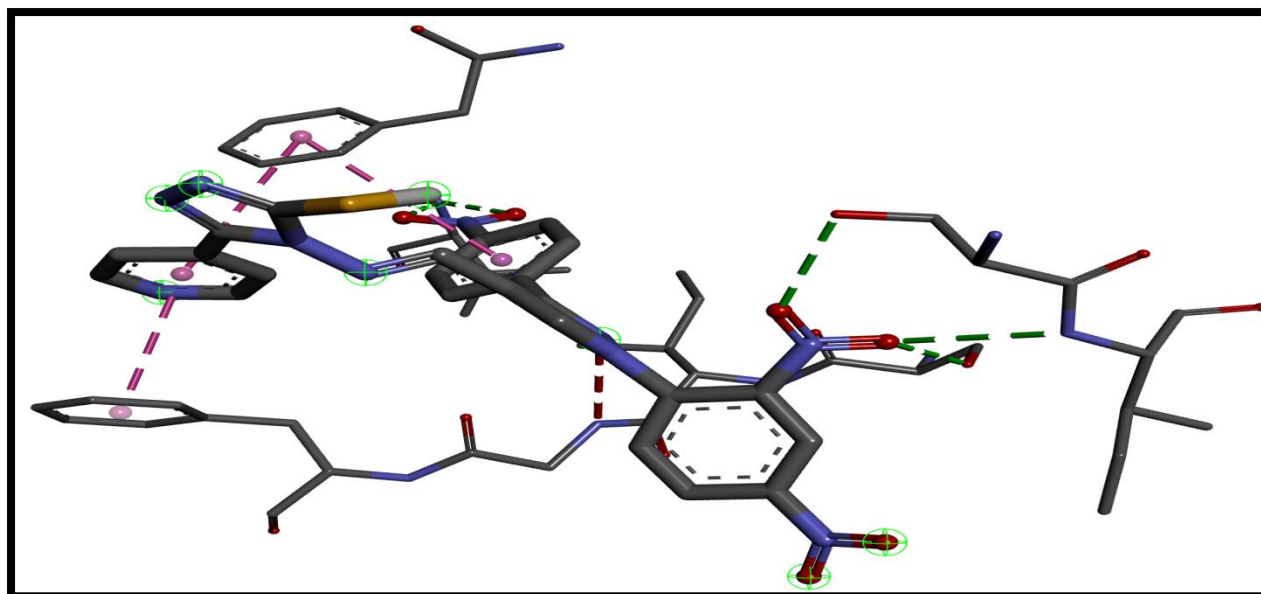


Figure-1. Binding interaction of Compound 21 against Mtb enoyl-reductase InhA (PDB 5JFO)

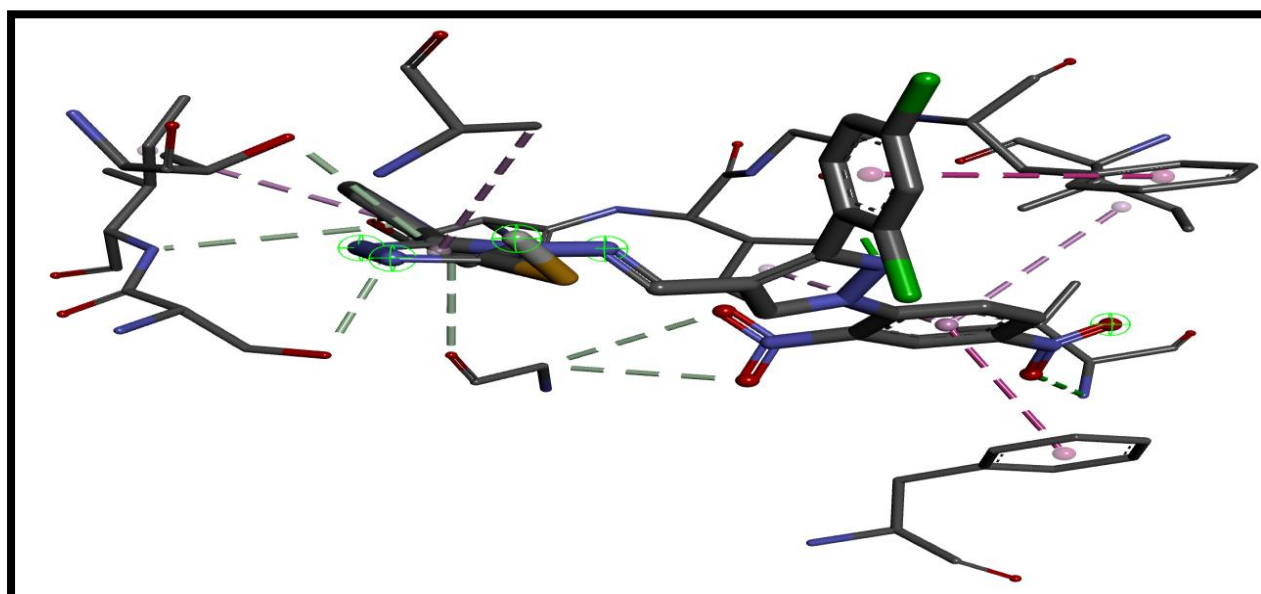


Figure 2. Binding interaction of Compound 05 against Mtb enoyl-reductase InhA (PDB 5JFO)

3.2. In-silico approach for ADME study and drug likeness prediction

The physical and chemical properties of a compounds are thoroughly examined to assess whether or not they satisfy criteria such as the Lipinski rule of five when evaluating how drug-like it is. Several parameters are taken into account, including topological polar surface area (TPSA), logP, hydrogen bond donors (HBD), number of rotatable bonds, molecular mass, molar refractivity, and hydrogen bond acceptors (HBA).

A summary of the findings is given in (Table 3), which shows that every derivative closely follows the Lipinski Rule of Five without any violations.

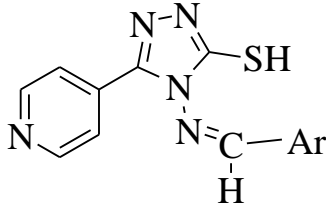
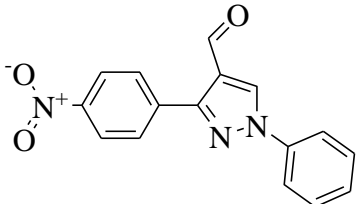
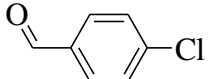
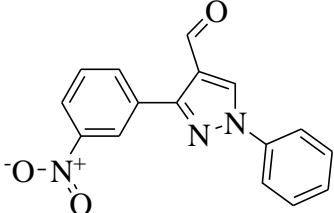
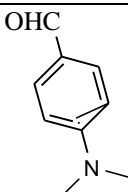
3.3. In silico pharmacokinetic and toxicity prediction-

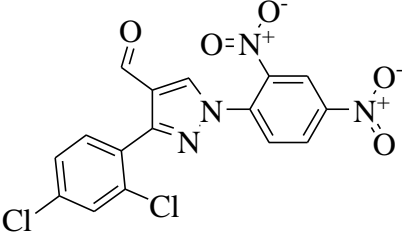
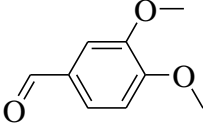
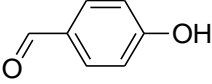
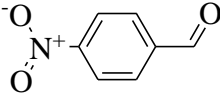
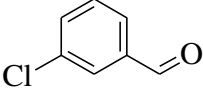
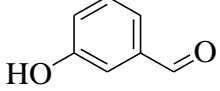
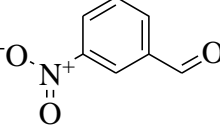
The pharmacokinetic and toxicity evaluation's findings, which are broken down in Tables (Table 4), demonstrated promising characteristics for each of the various metrics examined. Interestingly, high rates of intestinal absorption were demonstrated by all of the substances. Compounds showed remarkable 100% absorption. Nonetheless, three crucial factors were taken into account while analyzing their distribution: the distribution volume, permeability of the blood-brain barrier (BBB), and permeability of the central nervous system (CNS). The results showed that the compounds had a reasonable volume of distribution, pointing to a possible advantageous distribution of these compounds within the body.

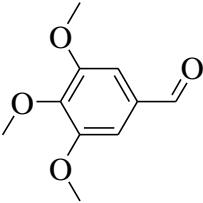
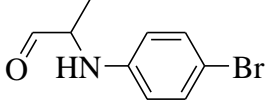
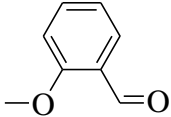
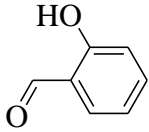
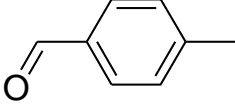
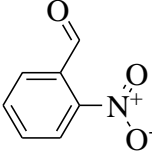
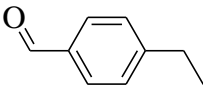
The compounds' low permeability through the BBB and CNS, however, suggests that their capacity to enter vital CNS regions is restricted. Additionally, the drugs' metabolic activity against important cytochrome P450 enzymes (CYPs) was assessed. The findings demonstrated that while each drug was inert against CYP2D6, it was active against CYP3A4, CYP1A2, CYP2C19, and CYP3A4. These results suggest that the chemicals that were produced have a substantial metabolic activity within the human body. The potential for effective metabolism was shown by the activity demonstrated against several CYP enzymes, which also improved the pharmacological profiles of these enzymes. The synthesized drugs showed intriguing results from the in silico toxicity assessment, despite their favorable pharmacokinetic properties.

All of the various compounds showed AMES toxicity, with the exception of some compounds. This suggested that these substances may have mutagenic qualities. On the other hand, synthetic substances are hepatotoxic and may be harmful to liver cells. Although the pharmacokinetic characteristics of these drugs are excellent, the reported toxicities raise serious concerns. By addressing these problems structurally, these chemicals' safety may be improved. In summary, these results underscore the significance of striking a balance between safety and efficacy, and they also point to the necessity of more chemical modification in order to attain lower toxicity.

Table 1: Newly designed pyridyl triazole derivatives.

 <p style="text-align: center;">General Structure</p>	
Compound Code	Ar
1.	 <p style="text-align: center;">3-(4-nitrophenyl)-1-phenyl-1H-pyrazole-4-carbaldehyde</p>
2.	 <p style="text-align: center;">p- chloro benzaldehyde</p>
3.	 <p style="text-align: center;">3-(3-nitrophenyl)-1-phenyl-1H-pyrazole-4-carbaldehyde</p>
4.	 <p style="text-align: center;">4-(dimethylamino)-3-methylbenzaldehyde</p>

5.	 <p>3-(2,4-dichlorophenyl)-1-(2,4-dinitrophenyl)-1H-pyrazole-4-carbaldehyde</p>
6.	 <p>3,4 di methoxy benzaldehyde</p>
7.	 <p>para hydroxyl benzaldehyde</p>
8.	 <p>p- nitro benzaldehyde</p>
9.	 <p>m- chloro benzaldehyde</p>
10.	 <p>m- hydroxy benzaldehyde</p>
11.	 <p>m- nitro benzaldehyde</p>

12.	 <p>3,4,5-tri methoxy benzaldehyde</p>
13.	 <p>2-(4-bromophenylamino)propanal</p>
14.	 <p>2-methoxy benzaldehyde</p>
15.	 <p>Salicylaldehyde</p>
16.	 <p>p- tolualdehyde</p>
17.	 <p>2-nitro benzaldehyde</p>
18.	 <p>4-ethyl benzaldehyde</p>

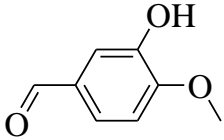
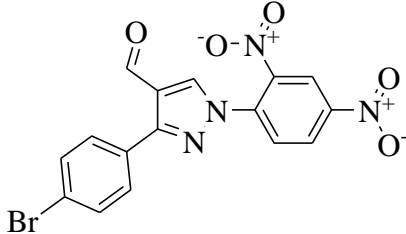
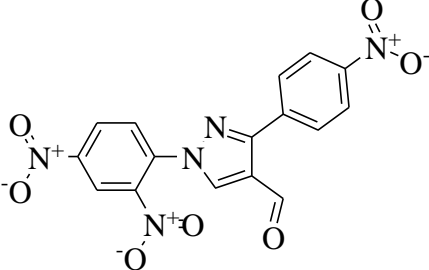
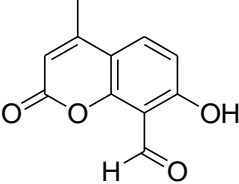
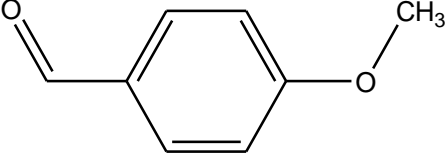
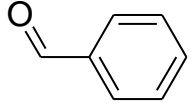
19.	 <p>Isovanilline</p>
20.	 <p>3-(4-bromophenyl)-1-(2,4-dinitrophenyl)-1H-pyrazole-4-carbaldehyde</p>
21.	 <p>1-(2,4-dinitrophenyl)-3-(4-nitrophenyl)-1H-pyrazole-4-carbaldehyde</p>
22.	 <p>7-hydroxy-4-methyl-2-oxo-2H-chromene-8-carbaldehyde</p>
23.	 <p>4-methoxybenzaldehyde</p>
24.	 <p>Benzaldehyde</p>

Table-2: Binding affinity along with binding interactions of designed compounds against Mtbenoyl-reductase InhA (PDB 5JFO)

Comp.Code	PDB ID	Binding Affinity	Interacting residues	Type of interaction	Distance
1.	5JFO	-9.7	THR 196	Conventional Hydrogen Bond	3.03
			SER 94		3.16
			ALA 22		3.29
			ILE 21		3.01, 3.36
			SER 20	Carbon Hydrogen bond	3.59
			ILE 95	Pi-Sigma	3.90
			PHE 41	Pi-Pi stacked	3.86
			ALA 198	Pi-Alkyl	4.05
			LEU 197		5.02
			Val 65		5.18
			ILE 122		4.82
2.	5JFO	-7.6	PHE 97	Pi-Pi stacked	4.33
			GLY 14	Pi-Sigma	3.37
			PHE 41	Pi-Alkyl	5.29
			ILE122		5.24
			ILE 16		4.91
			ILE 95		4.96
3.	5JFO	-9.4	SER 94	Conventional Hydrogen Bond	3.02
			THR 196		3.18
			ILE 85	Pi-Sigma	3.81
			PHE 41	Pi-Pi stacked	3.97
			ILE 122	Pi-Alkyl	4.69
			VAL 65		5.28
			ALA 198		4.47
			ILE 16		5.18
4.	5JFO		GLY 96	Carbon Hydrogen bond	3.53
			GLY 14	3.31	
			ILE 95	Pi-Sigma	3.98
			PHE 41	Pi-Pi stacked	4.86
			PHE 97		3.99
			VAL 65	Pi-Alkyl	5.42
			5.	5JFO	-10.1
GLY 96	3.14				

			VAL 65	Hydrogen Bond	2.71
			ILE 21	Carbon	3.89
			SER 20	Hydrogen bond	4.11
			THR 196	Pi Donor Hydrogen Bond	3.61
			PHE 41	Pi-Pi	4.10
			PHE 97	stacked	4.85
			ILE 95		5.26
			ILE 122	Pi-Alkyl	4.72
			ALA 198		4.81
			SER 94	Conventional Hydrogen Bond	3.12
			ASP 64	Carbon Hydrogen bond	3.34
6.	5JFO	-7.1	ILE 16	Pi-Sigma	3.57
			PHE 41	Pi-Pi stacked	4.66
			ILE 122		4.15
			ILE 95	Pi-Alky	5.25
			VAL 65		4.32, 4.80
					4.45
			LYS 118	Conventional Hydrogen Bond	3.07
			GLY 14	Carbon Hydrogen bond	3.69
7.	5JFO	-7.9	ILE 95	Pi-Sigma	3.88
			PHE 97		3.87
			PHE 41	Pi-Pi stacked	4.38
			VAL 65	Pi-Alkyl	5.11
			SER 94	Conventional	3.18
			VAL 65	Hydrogen Bond	3.10, 3.31
			GLY 96	Carbon Hydrogen bond	3.41
8.	5JFO	-7.9	ILE 95	Pi-Sigma	3.82
			PHE 41	Pi-Pi stacked	4.52
			ILE 122	Pi-Alkyl	5.35

9.	5JFO	-7.7	GLY 14	Carbon	3.37
			SER 94	Hydrogen bond	3.38
			ILE 16	Pi-Sigma	3.91
			ILE 95		3.84
			PHE 41	Pi Sulfur	5.19
			ILE 16	Pi-Alkyl	3.91
VAL95	3.84				
10.	5JFO	-7.7	ASP 64	Conventional Hydrogen Bond	2.20
			ILE 95	Pi-Sigma	3.70
			PHE 41	Pi-Pi stacked	4.08
			ILE 122	Pi-Alkyl	4.89
			VAL 65		5.15
11.	5JFO	-8.2	SER 94	Conventional Hydrogen Bond	3.32
			THR 39	Hydrogen Bond	3.03
			GLY 14		3.08
			SER 13	Carbon Hydrogen bond	3.51
			ILE 95	Pi-Sigma	3.90
			ILE 16		3.55
			PHE 41		Pi-Pi stacked
12.	5JFO	-7.1	LYS 118	Conventional Hydrogen Bond	3.89
			ILE 95	Pi-Sigma	3.68
			PHE 41	Pi-Pi Stacked	5.35
			PHE 97		3.86
			VAL 65	Pi-Alkyl	5.09
13.	5JFO	-7.2	SER 20	Conventional Hydrogen Bond	2.91
			THR 196	Hydrogen Bond	3.66
			ILE 16		Pi-Sigma
			PHE 97	Pi-Pi Stacked	4.21
			GLY 14		4.33
			ILE 95		5.12
			ILE 122	Pi-Alkyl	5.08
PHE 41	4.68				
14.	5JFO	-7.8	GLY 14	Carbon Hydrogen bond	3.57
			ILE 95	Pi-Sigma	3.91

			PHE 41		4.46
			PHE 97	Pi-Pi Stacked	3.86
			VAL 65	Pi-Alkyl	5.12
			GLY 96	Conventional Hydrogen Bond	2.29
15.	5JFO	-7.5	ILE 95	Pi-Sigma	3.99
			PHE 41	Pi-Pi Stacked	3.79
			PHE 41	Pi-Pi T Shaped	5.31
			ILE 16		4.61, 4.61
			ILE 122	Pi-Alkyl	4.75
			VAL 65		5.13
			ILE 95	Carbon Hydrogen bond	4.74
16.	5JFO	-8.0	GLY 14	Hydrogen bond	3.20
			GLY 96	Pi- Donor Hydrogen Bond	4.06
			PHE 97	Pi-Sigma	3.99
			PHE 41	Pi-Pi Stacked	4.87
			VAL 65	Pi-Alkyl	5.48
			GLY 14	Carbon Hydrogen bond	3.69
17.	5JFO	-8.0	ILE 95	Pi-Sigma	3.74
			PHE 97		3.78
			PHE 41	Pi-Pi Stacked	5.29
			ILE 16		5.19
			VAL 65	Pi-Alkyl	5.33
			SER 94	Conventional Hydrogen Bond	3.18
18.	5JFO	-7.9	GLY 14	Carbon Hydrogen bond	3.45
			ILE 16		3.96
			ILE 95	Pi-Sigma	3.95
			PHE 41	Pi-Pi Stacked	4.60
			VAL 65		4.50
			ILE 122	Pi-Alkyl	3.87
19.	5JFO	-7.6	SER 94	Conventional Hydrogen Bond	2.96, 2.57
			GLY 96	Carbon	3.69

			Hydrogen bond		
			GLY 14	Pi-Sigma	3.83
			PHE 41	Pi-Pi Stacked	5.56
			ILE 16		5.27
			ILE 21	Pi-Alkyl	4.10
			ILE 95		5.14
			MET 147		4.17
			SER 94	Conventional	3.34
			GLY 96	Hydrogen Bond	3.14
			VAL 65		2.73
			ILE 21	Carbon	4.09
			SER 20	Hydrogen bond	3.87
20.	5JFO	-10	THR 196	Pi-Donor Hydrogen Bond	3.59
			GLY 14		3.72
			PHE 97	Pi-Pi Stacked	4.87
			PHE 41	Pi-Pi T Shaped	4.12
			ILE 95		5.27
			ILE 122	Pi-Alkyl	4.71
			ALA 198		4.78
			ILE 21	Conventional Hydrogen Bond	3.33
			ILE 20		2.91
			SER 94		3.24
21.	5JFO	-10.2	VAL 65		3.30
			ILE 95	Pi- Sigma	3.46
			PHE 97	Pi-Pi Stacked	3.84
			PHE 41	Pi-Pi T Shaped	4.95
			SER 94	Conventional Hydrogen Bond	3.05
			ILE 95	Pi- Sigma	3.71
22.	5JFO	-9.3	ILE 122		3.82
			PHE 41	Pi-Pi Stacked	5.44, 4.21, 3.67
			ILE 16	Pi-Alkyl	4.58
			VAL 65		5.37
			LYS 118	Conventional Hydrogen Bond	3.06
23.	5JFO	-7.9	GLY 14	Carbon	3.47

			Hydrogen bond		
			ILE 95	Pi- Sigma	4.48
			PHE 41	Pi-Pi Stacked	4.67
			PHE 97		3.84
			ILE 16	Pi-Alkyl	4.90
			VAL 65		5.43
			ILE 95	Pi- Sigma	3.91
			PHE 41	Pi-Pi Stacked	5.17
			PHE 97		3.87
			ILE 16	Pi-Alkyl	4.81

24.	5JFO	-7.9	ILE 95	Pi- Sigma	3.91
			PHE 41	Pi-Pi Stacked	5.17
			PHE 97		3.87
			ILE 16	Pi-Alkyl	4.81

Table 3: Predicted physicochemical properties, lipophilicity, solubility, and drug-likeness of the identified 24 compounds ²⁵⁻²⁸.

Comp d.	MW(g/mol)	nRot	mlog P	HB A	HB D	MR	TPSA	Lipinski's violation	Ghose violations	Vebers violation
1.	469.5	6	3.17	7	1	129.74	162.24	0	0	1
2.	315.78	3	2.95	4	0	84.95	94.76	0	0	0
3.	469.5	6	3.17	7	1	129.74	162.24	0	0	1
4.	324.4	4	1.98	4	0	94.15	98	0	0	0
5.	584.39	7	3.08	9	2	147	211.9	0	3	1
6.	341.39	5	1.45	6	0	92.92	113.22	0	0	0
7.	297.34	3	1.48	5	1	81.96	114.99	0	0	0
8.	327.34	4	1.92	6	1	87.18	144.42	0	0	1
9.	315.78	3	2.95	4	0	84.95	94.76	0	0	0
10.	297.34	3	1.48	5	1	81.96	114.99	0	0	0
11.	327.34	4	1.92	6	1	87.18	144.42	0	0	1
12.	371.41	6	1.18	7	0	99.41	122.45	0	0	0
13.	389.27	4	2.92	4	1	96.79	106.79	0	0	0
14.	311.36	4	1.74	5	0	86.43	103.9	0	0	0

							9			
15.	297.34	3	1.48	5	1	81.96	114.9 9	0	0	0
16.	295.36	3	2.28	4	0	84.9	94.76	0	0	0
17.	327.34	4	1.92	6	1	87.18	144.4 2	0	0	1
18.	309.39	4	2.53	4	0	89.71	94.76	0	0	0
19.	327.36	4	1.2	6	1	88.45	124.2 2	0	0	0
20.	594.4	7	2.71	9	2	144.6 8	211.9	2	3	1
21.	561.51	8	1.67	11	3	144.2 2	261.5 6	2	2	1
22.	379.39	3	1.71	7	1	102.9 7	145.2	0	0	1
23.	311.36	4	1.74	5	0	86.43	103.9 9	0	0	0
24.	281.34	3	2.43	4	0	79.94	94.76	0	0	0

Table 4: Predicted ADMET properties of the identified 24 hits by using pkCSM server [25-28]

Comp.	Absorption	Distribution			Metabolism							Excretion	Toxicity	
	Intestinal absorption (human)	Vds (human)	Bbb permeability	Cns permeability	Substrate		Inhibitors					Total Clearance	AMES toxicity	Hepatotoxicity
	numeric (% absorbed)	numeric (log L kg ⁻¹ n)	numeric (log BB)	numeric (log PS)	2D 6	3A 4	1A 2	2C1 9	2C 9	2D 6	3A 4	Numeric (log ml/min/kg)	Categorical (Yes/No)	Categorical (Yes/No)
1.	100	0.195	-1.634	-2.502	No	Yes	No	Yes	Yes	No	NO	0.212	Yes	Yes
2.	94.343	-0.763	0.03	-2.07	No	Yes	Yes	Yes	No	No	No	0.083	No	Yes
3.	98.998	-1.422	-1.23	-2.025	No	Yes	No	Yes	Yes	NO	Yes	0.351	Yes	Yes
4.	96.401	-0.715	-0.016	-2.276	No	Yes	Yes	No	No	No	No	0.186	No	Yes
5.	98.376	-1.626	-2.096	-1.983	No	Yes	No	Yes	Yes	No	Yes	0.305	No	Yes

6.	95.996	-1	-0.821	-2.513	No	Yes	Yes	No	No	No	No	0.319	Yes	Yes
7.	93.119	-0.909	-0.589	-2.375	No	Yes	Yes	No	No	No	No	-0.018	Yes	No
8.	89.296	-1.053	-0.893	-2.373	No	Yes	Yes	No	No	No	No	0.115	Yes	Yes
9.	94.343	-0.763	0.03	-2.07	No	Yes	Yes	Yes	No	No	No	0.088	No	Yes
10.	93.119	-0.909	-0.589	-2.375	No	Yes	Yes	No	No	No	No	0.102	Yes	Yes
11.	89.296	-1.053	-0.893	-2.373	No	Yes	Yes	No	No	No	No	0.293	Yes	Yes
12.	95.993	-1.134	-1.049	-3.095	No	Yes	Yes	No	No	No	No	0.565	No	Yes
13.	90.333	90.333	-0.701	-2.026	No	Yes	Yes	Yes	No	No	No	-0.189	No	Yes
14.	96	-0.864	-0.098	-2.349	No	Yes	Yes	No	No	No	No	0.311	Yes	Yes
15.	93.119	-0.909	-0.589	-0.589	No	Yes	Yes	No	No	No	No	0.162	Yes	Yes
16.	95.801	-0.695	-0.695	-2.111	No	Yes	Yes	Yes	No	No	No	0.157	No	Yes

17.	89.296	-1.053	-0.893	-2.373	No	Yes	Yes	No	No	No	No	0.315	Yes	Yes
18.	95.692	-0.639	0.027	-2.135	No	Yes	Yes	Yes	No	No	No	0.121	No	Yes
19.	93.115	-1.046	-0.817	-2.539	No	Yes	Yes	No	No	No	No	0.169	Yes	Yes
20.	96.936	-1.613	-1.936	-2.075	No	Yes	No	Yes	Yes	No	No	0.283	Yes	Yes
21.	93.049	-1.749	-2.288	-2.401	No	Yes	No	Yes	Yes	No	Yes	0.341	Yes	Yes
22.	88.412	-1.26	-0.928	-2.33	No	Yes	No	No	No	No	No	-0.004	No	Yes
23.	96	-0.864	-0.098	-2.349	No	Yes	Yes	No	No	No	No	0.129	Yes	Yes
24.	96.003	-0.726	0.031	-2.185	No	No	Yes	No	No	No	No	0.216	Yes	Yes

Conclusion-

This *in silico* study delved into the molecular interactions between potential compounds and the Mt enoyl-reductaseInhA (PDB 5JFO) which is a crucial target in TB therapy. Compound 21 emerged with the highest negative binding affinity (-10.2 kcal/mol) further followed closely by compound 5 (-10.1 kcal/mol) and found exhibiting promising interactions within the active site of enoyl-reductaseInhA. The elucidation of these compound-target interactions via docking studies contributes significantly to rational drug design. It will offer insights crucial for refining hit compounds and ultimately fostering the creation of more effective treatments against TB.

The chosen ligands with higher binding affinities showed zero violations of Lipinski rules with similar bioavailability and a high rate of gastrointestinal absorption in the drug-likeness and pharmacokinetic profile prediction results. On the other hand, toxicity parameters like carcinogenicity and cytotoxicity were all predicted as non-toxic (inactiveness). The majority of the designed compounds have lead-like characteristics and ADMET values that fall within an acceptable range.

Conflict of interest:

The authors have declared no conflict of interest.

Financial support and sponsorship:

Nil.

Acknowledgement

We would like to thank Government College of Pharmacy, Karad, District- Satara, Maharashtra, for giving the resources needed to finish this research. The authors would like to thank Dr. M. S. Charde, my guide, for his guidance and technical support.

References-

1. Villar-Hernández R, Ghodousi A, Konstantynovska O, Duarte R, Lange C, Raviglione M. Tuberculosis: current challenges and beyond, *Breathe*. 2023; 9: 220166. <https://doi.org/10.1183/20734735.0166-2022>.
2. Kremer L, Gue Y, Gurcha SS, Loch C, Besra GS. Temperature-induced changes in the cell-wall components of *Mycobacterium thermoresistibile*, *Microbiology* (N Y). 2002; 148: 3145–3154.
3. Koul A, Arnoult E, Lounis N, Guillemont J, Andries K. The challenge of new drug discovery for tuberculosis, *Nature*. 2011; 469: 483–490. <https://doi.org/10.1038/nature09657>.
4. Glynn JR, Khan P, Mzembe T, Sichali L, Fine PEM, Crampin AC, Houben RMGJ. Contribution of remote *M.tuberculosis* infection to tuberculosis disease: A 30-year population study, *PLoS One*. 2023; 18: e0278136. <https://doi.org/10.1371/JOURNAL.PONE.0278136> .
5. Williams CM, Muhammad AK, Sambou B, Bojang A, Jobe A, Daffeh GK, Owolabi O, Pan D, Pareek M, Barer MR, Sutherland JS, Haldar P. Exhaled *Mycobacterium tuberculosis* Predicts Incident Infection in Household Contacts, *Clinical Infectious Diseases*. 2023; 76: e957–e964. <https://doi.org/10.1093/CID/CIAC455> .
6. Masini T, Furin J, Udwardia Z, Guglielmetti L. Optimal management of drug-resistant tuberculosis: Can India lead the way?, *Indian Journal of Medical Research*. 2023; 157: 220–222. https://doi.org/10.4103/ijmr.ijmr_300_23 .
7. Singh M, Jeyaraman M, Jeyaraman N, Jayakumar T, Iyengar KP, Jain VK. *Mycobacterium Tuberculosis* infection of the wrist joint: A current concepts review, *J ClinOrthop Trauma*. 2023; 44: 102257. <https://doi.org/10.1016/J.JCOT.2023.102257> .

8. Mancuso G, Midiri A, De Gaetano S, Ponzio E, Biondo C. Tackling Drug-Resistant Tuberculosis: New Challenges from the Old Pathogen *Mycobacterium tuberculosis*. *Microorganisms*. 2023; 11: 2277. <https://doi.org/10.3390/MICROORGANISMS11092277> .
9. Walsh TR, Gales AC, Laxminarayan R, Dodd PC. Antimicrobial Resistance: Addressing a Global Threat to Humanity, *PLoS Med*. 2023; 20: e1004264. <https://doi.org/10.1371/JOURNAL.PMED.1004264> .
10. Pattnaik M, Pattnaik S, Pradhan J, Bhattacharya D. Antimicrobial resistance and its possible implications in the future: a mini review, *Int J Community Med Public Health*. 2023; 10: 4485–4491. <https://doi.org/10.18203/2394-6040.ijcmph20233499> .
11. Alcaraz M, Edwards TE, Kremer L. New therapeutic strategies for *Mycobacterium abscessus* pulmonary diseases – untapping the mycolic acid pathway, *Expert Rev Anti Infect Ther*. 2023; 21: 813–829. <https://doi.org/10.1080/14787210.2023.2224563> .
12. Bussi C, Gutierrez MG. *Mycobacterium tuberculosis* infection of host cells in space and time, *FEMS Microbiol Rev*. 2019; 43: 341–361. <https://doi.org/10.1093/FEMSRE/FUZ006>.
13. Marrakchi H, Lanéelle MA, Daffé M. Mycolic acids: Structures, biosynthesis, and beyond, *Chem Biol*. 2014; 21: 67–85. <https://doi.org/10.1016/j.chembiol.2013.11.011>.
14. Takayama K, Wang C, Besra GS. Pathway to synthesis and processing of mycolic acids in *Mycobacterium tuberculosis*. *Clin Microbiol Rev*. 2005;18(1): 81-101. doi: 10.1128/CMR.18.1.81-101.2005.
15. Kumar G, Kapoor S. Targeting mycobacterial membranes and membrane proteins: Progress and limitations, *Bioorg Med Chem*. 2023; 81: 117212. <https://doi.org/10.1016/J.BMC.2023.117212> .
16. Zonon NF, Mousse LM, Allangba KNPG, Kouman KC, Megnassan E. Molecular Modeling of Enoyl Acyl Carrier Protein Reductase Inhibitors for *Mycobacterium tuberculosis* and their

- Pharmacokinetic Predictions. *J Pharm Res Int.* 2023; 35: 1–27.
<https://doi.org/10.9734/JPRI/2023/V35I287446> .
17. Rathod S, Chavan P, Mahuli D, Rochlani S, Shinde S, Pawar S, Choudhari P, Dhavale R, Mudalkar P, Tamboli F. Exploring biogenic chalcones as DprE1 inhibitors for antitubercular activity via in silico approach, *J Mol Model.* 2023; 29: 1–23.
<https://doi.org/10.1007/S00894-023-05521-8> .
18. Rathod S, Shinde K, Porlekar J, Choudhari P, Dhavale R, Mahuli D, Tamboli Y, Bhatia M, Haval KP, Al-Sehemi AG, Pannipara M. Computational Exploration of Anti-cancer Potential of Flavonoids against Cyclin-Dependent Kinase 8: An In Silico Molecular Docking and Dynamic Approach. *ACS Omega.* 2022;8: 391–409.
<https://doi.org/10.1021/acsomega.2c04837> .
19. Hunter AD. ACD/ChemSketch 1.0 (freeware); ACD/ChemSketch 2.0 and its Tautomers, Dictionary, and 3D Plug-ins; ACD/HNMR 2.0; ACD/CNMR 2.0, *J Chem Educ.* 1997; 74(8): 905-908.
20. Alamri MA, Tahir Ul Qamar M, Afzal O, Alabbas AB, Riadi Y, Alqahtani SM. Discovery of anti-MERS-CoV small covalent inhibitors through pharmacophore modeling, covalent docking and molecular dynamics simulation. *J Mol Liq.* 2021; 330:115699. doi: 10.1016/j.molliq.2021.115699.
21. Snyder HD, Kucukkal TG. Computational Chemistry Activities with Avogadro and ORCA, *J Chem Educ.* 2021; 98: 1335–1341. <https://doi.org/10.1021/acs.jchemed.0c00959> .
22. Bakale RD, Sulakhe SM, Kasare SL, Sathe BP, Rathod SS, Choudhari PB, MadhuRekha E, Sriram D, Haval KP. Design, synthesis and antitubercular assessment of 1, 2, 3-triazole incorporated thiazolylcarboxylate derivatives, *Bioorg Med ChemLett.* 2023; 97: 129551.
<https://doi.org/10.1016/j.bmcl.2023.129551> .

23. Berman HM, Westbrook J, Feng Z, Gilliland G, Bhat TN, Weissig H, Shindyalov IN, Bourne PE. The Protein Data Bank, *Nucleic Acids Res.* 2000; 28: <https://doi.org/doi.org/10.1093/nar/28.1.235> .
24. Gaikwad R, Rathod S, Shinde A. In-silico Study of Phytoconstituents from *Tribulusterrestris* as potential Anti-psoriatic agent, *Asian Journal of Pharmaceutical Research.* 2022; 12: 267–274. <https://doi.org/10.52711/2231-5691.2022.00043>.
25. Bansode P, Pore D, Tayade S, Patil S, Choudhari P, Rashinkar G. Remarkable anti-breast cancer activity and molecular docking studies of ferrocene tethered pyrimidobenzothiazoles and pyrimidobenzimidazoles, *Results Chem.* 2023; 5: <https://doi.org/10.1016/j.rechem.2022.100758> .
26. Al-Sehemi AG, Pannipara M, Parulekar RS, Kilbile JT, Choudhari PB, Shaikh MH. In silico exploration of binding potentials of anti SARS-CoV-1 phytochemicals against main protease of SARS-CoV-2, *Journal of Saudi Chemical Society.* 2022; 26: <https://doi.org/10.1016/j.jscs.2022.101453> .
27. Basha GM, Parulekar RS, Al-Sehemi AG, Pannipara M, Siddaiah V, Kumari S, Choudhari PB, Tamboli Y. Design and in silico investigation of novel Maraviroc analogues as dual inhibition of CCR-5/SARS-CoV-2 Mpro, *J Biomol. Struct. Dyn.* 2022; 40(21): 11095-11110. <https://doi.org/10.1080/07391102.2021.1955742> .
28. Dey S, Rathod S, Gumphalwad K, Yadav N, Choudhari P, Rajakumara E, Dhavale R, Mahuli D. Exploring α , β -unsaturated carbonyl compounds against bacterial efflux pumps via computational approach, *J Biomol.Struct. Dyn.* 2023; 1–14. <https://doi.org/10.1080/07391102.2023.2246568> .
29. Rathod S, Bhande D, Pawar S, Gumphalwad K, Choudhari P, More H. Identification of Potential Hits against Fungal Lysine Deacetylase Rpd3 via Molecular Docking, *Molecular*

Dynamics Simulation, DFT, In-Silico ADMET and Drug-Likeness Assessment, Chemistry Africa. 2023. <https://doi.org/10.1007/s42250-023-00766-5> .

30. Al-Sehemi AG, Pannipara M, Parulekar RS, Patil O, Choudhari PB, Bhatia MS, Zubaidha PK, Tamboli Y. Potential of NO donor furoxan as SARS-CoV-2 main protease (Mpro) inhibitors: in silico analysis, *J Biomol. Struct. Dyn.* 2020: 1–15. <https://doi.org/10.1080/07391102.2020.1790038> .
31. Rathod S, Dey S, Pawar S, Dhavale R, Choudhari P, Rajakumara E, Mahuli D, Bhagwat D, Tamboli Y, Sankpal P, Mali S, More H. Identification of potential biogenic chalcones against antibiotic resistant efflux pump (AcrB) via computational study. *J Biomol. Struct. Dyn.* 2023; 1–19. <https://doi.org/10.1080/07391102.2023.2225099> .
32. Rochlani S, Bhatia M, Rathod S, Choudhari P, Dhavale R. Exploration of limonoids for their broad spectrum antiviral potential via DFT, molecular docking and molecular dynamics simulation approach, *Nat Prod Res.* 2023; 1–6. <https://doi.org/10.1080/14786419.2023.2202398> .
33. Ramos DF, Leitão GG, Costa F, Das N, Abreu L, Villarreal JV, Leitão SG. Investigation of the Antimycobacterial activity of 36 Plant extracts from the Brazilian Atlantic Forest. *Brazilian J Pharm Sci.* 2008; 44: 669-674.
34. Martin A, Portaels F, Palomino JC: Colorimetric Redox-Indicator Methods for the Rapid Detection of Multidrug resistance in Mycobacterium tuberculosis: A Systematic Review and Meta-analysis. *J Antimicrob Chemother.* 2007; 59:175–183.
35. Dallakyan S, Olson AJ. Small-molecule library screening by docking with PyRx, *Methods in Molecular Biology.* 2015; 1263: 243–250. https://doi.org/10.1007/978-1-4939-2269-7_19.
36. Marrakchi H, Laneelle G, Quemard A. InhA, a target of the antituberculous drug isoniazid, is involved in a mycobacterial fatty acid elongation system, FAS-II, *Microbiology (N Y).* 2000; 146: 289–296.

37. Sabbah M, Mendes V, Vistal RG, Dias DMG, Záhorszka M, Mikušová K, Korduláková J, Coyne AG, Blundell TL, Abell C. Fragment-based design of *Mycobacterium tuberculosis* InhA inhibitors, J Med Chem. 2020; 63: 4749–4761. <https://doi.org/10.1021/acs.jmedchem.0c00007> .
38. He X, Alian A, Ortiz de Montellano PR. Inhibition of the *Mycobacterium tuberculosis* enoyl acyl carrier protein reductase InhA by arylamides. Bioorg Med Chem. 2007; 15: 6649–6658. <https://doi.org/10.1016/j.bmc.2007.08.013> .
39. Kanetaka H, Koseki Y, Taira J, Umei T, Komatsu H, Sakamoto H, Gulten G, Sacchetti JC, Kitamura M, Aoki S. Discovery of InhA inhibitors with anti-mycobacterial activity through a matched molecular pair approach, Eur J Med Chem. 2015; 94: 378–385. <https://doi.org/10.1016/j.ejmech.2015.02.062> .